Carbohydrate Polymers 92 (2013) 830–841

Contents lists available at SciVerse ScienceDirect

Carbohydrate Polymers

journal homepage: www.elsevier.com/locate/carbpol

Chemical and functional properties of cell wall polymers from two cherry varieties at two developmental stages

María F. Basanta [a], Marina F. de Escalada Plá [b], Carlos A. Stortz [a,*], Ana M. Rojas [b]

[a] Departamento de Química Orgánica-CIHIDECAR, Facultad de Ciencias Exactas y Naturales, Universidad de Buenos Aires, Ciudad Universitaria, 1428 Buenos Aires, Argentina
[b] Departamento de Industrias, Facultad de Ciencias Exactas y Naturales, Universidad de Buenos Aires, Ciudad Universitaria, 1428 Buenos Aires, Argentina

ARTICLE INFO

Article history:
Received 4 July 2012
Received in revised form
14 September 2012
Accepted 28 September 2012
Available online 8 October 2012

Keywords:
Sweet cherry
Cell wall biopolymers
Polysaccharides
Ripening
Functional properties
Firmness

ABSTRACT

The cell wall polysaccharides of Regina and Sunburst cherry varieties at two developmental stages were extracted sequentially, and their changes in monosaccharide composition and functional properties were studied. The loosely-attached pectins presented a lower D-galacturonic acid/rhamnose ratio than ionically-bound pectins, as well as lower thickening effects of their respective 2% aqueous solution: the lowest Newtonian viscosity and shear rate dependence during the pseudoplastic phase. The main constituents of the cell wall matrix were covalently bound pectins (probably through diferulate cross-linkings), with long arabinan side chains at the RG-I cores. This pectin domain was also anchored into the XG-cellulose elastic network. Ripening occurred with a decrease in the proportion of HGs, water extractable GGM and xylogalacturonan, and with a concomitant increase in neutral sugars.

Ripening was also associated with higher viscosities and thickening effects, and to larger distribution of molecular weights. The highest firmness and compactness of Regina cherry may be associated with its higher proportion of calcium-bound HGs localized in the middle lamellae of cell walls, as well as to some higher molar proportion of NS (Rha and Ara) in covalently bound pectins. These pectins showed significantly better hydration properties than hemicellulose and cellulose network. Chemical composition and functional properties of cell wall polymers were dependent on cherry variety and ripening stage, and helped explain the contrasting firmness of Regina and Sunburst varieties.

© 2012 Elsevier Ltd. All rights reserved.

1. Introduction

Cherry is a fleshy stone fruit of trees of some species of the genus *Prunus*. Sweet cherries (*Prunus avium* L.) are commercially cultivated in more than 40 countries worldwide. The world production of sweet cherry in 2011/2012 is forecast at 1.9 million metric tons. The highest share is held by Turkey (22%), followed closely by USA, Iran and Italy. Individual participation of other countries is below 5% (USDA, 2011). The Southern hemisphere (mainly Chile, South Africa, Australia and Argentina) contributes to only 3.5% of the world production. In spite of this small proportion, it is important economically for local development because of harvest and counter-season marketing advantages (Cittadini, 2007). Consumers can now find cherries throughout the year: in November and December they can be picked up in Argentina, Chile, Australia and New Zealand. In Argentina, Regina and Sunburst are among the cherry varieties grown, being very productive. Regina needs to be pollinated and Sunburst is one of the suitable pollinators (Cittadini, 2007). Regina cherry is characterized by a firm and compact mesocarp, whereas Sunburst is the softest cherry grown in Argentina. Size, absence of misshapen fruit, freedom of cracks, green fleshy stems together with high soluble solids, and red surface color, are the main quality attributes of fresh cherries (Mattheis & Fellman, 2004). The cell wall decisively contributes to the texture of vegetable foods because it supports the turgor pressure due to its elasticity and mechanical resistance (Jarvis, 2011). These characteristics are due to the chemical composition and functional properties (rheological performance, hydration properties) of the polymers that constitute the cell walls (Chanliaud, Burrows, Jeronimidis, & Gidley, 2002; Toivonen & Brummell, 2008). Some partial investigations of the cell wall changes occurring during cherry ontogeny were published (Batisse, Buret, & Coulomb, 1996; Fils-Lycaon & Buret, 1990). As occurs with other fruit species, pectins become more soluble, the RG-I side chains are removed (Kondo & Danjo, 2001) and wall degrading enzymes (pectin methyl esterase, polygalacturonase, and β-galactosidase) appear to be involved in the softening process (Andrews & Shulin, 1995; Barrett & Gonzalez, 1994; Fils-Lycaon & Buret, 1990).

Chemical changes of cell wall polymers related to ripening alter their functionality and, hence, fruit firmness. The functional properties of the cell wall biopolymers are also relevant in the upgrading of vegetable by-products. By sequential extraction of

* Corresponding author. Tel.: +54 11 4576 3346; fax: +54 11 4576 3346.
E-mail address: stortz@qo.fcen.uba.ar (C.A. Stortz).

0144-8617/$ – see front matter © 2012 Elsevier Ltd. All rights reserved.
http://dx.doi.org/10.1016/j.carbpol.2012.09.091

the polymers from the cell wall material isolated from Regina and Sunburst cherry varieties it is possible to ascertain the chemical composition and polymer interactions within the cell walls (Fry, 1986; Koh & Melton, 2002), as already studied by Ponce, Ziegler, Stortz, and Sozzi (2010) for a related fleshy stone fruit like Japanese plum (*Prunus salicina* Lindl.). They found that arabinose was the main neutral monosaccharide constituent in cell walls of Japanese plum during growth and the most dynamic neutral sugar in pectic fractions. Arabinose loss from tightly bound pectins was a relatively early feature in the sequence of cell wall biochemical modifications, thus suggesting a softening-related role during on-tree ripening. Rosli, Civello, and Martínez (2004) studied three strawberry (*Fragaria* × *ananassa* Duch.) cultivars with different softening rates by sequential extraction, and determined that the fleshy fruit softens during ripening mainly as a consequence of solubilization and depolymerization of cell wall components, showing differences among cultivars only in immature stages. After sequential extraction of cell wall polysaccharides, Peña and Carpita (2004) determined that loss of highly branched arabinans and debranching of RG-I accompanied the loss in firmness and cell separation during apple (*Malus domestica* Borkh) storage. The functional characterization of the biopolymer fractions sequentially dissolved or remaining at each extractive step can also contribute to understand their biological performance and ripening-related changes, as well as to predict the potential usefulness of the biopolymers extracted from sweet cherry in view of residue upgrading. This work aims to determine the cell wall polymer changes associated with the ripening of two sweet cherry varieties with contrasting firmness, and simultaneously evaluate the rheological performance of the soluble fractions and the hydration properties of the insoluble residues isolated at some steps of the sequential extraction of cell wall biopolymers, in order to understand better the ripening process and their biological functionality.

2. Materials and methods

2.1. Plant material

Cherry fruits cvs. Regina and Sunburst were picked up from trees located in the Río Negro Upper Valley, Argentina (39°01′32″S, 67°44′22″W, 240 m above sea level). Ca. 1.5 kg of each were collected at two different developmental stages, unripe (Regina 47 DAA, Sunburst 49 DAA) and ripe (85 DAA for both varieties).

2.2. Cell wall preparation and fractionation

Cell wall preparation was performed as previously described (Ponce et al., 2010): after removal of endocarp (when possible) and peduncle, 500 g of fruit was put into 2 L of ice-cold 80% (v/v) ethanol and homogenized in a Warring blender and in an Omni Mixer homogenizer. The homogenate was boiled for 30 min, cooled, and filtered through glass filter paper (Whatman GF/C). The retentate was thoroughly washed with 95% (v/v) ethanol. The solids were then resuspended in 2 L of chloroform:methanol (1:1), stirred for 15 min and filtered. The retentate was washed with the same solvent mixture. The insoluble material was washed with acetone, yielding the crude cell wall extract (alcohol insoluble residue, AIR). The AIR was air-dried in a hood and in a vacuum desiccator overnight and then weighed.

Cell wall fractionation was performed as previously described (Ponce et al., 2010) and it is shown in Scheme 1. Briefly, 12 g of AIR was stirred for 4 h at room temperature with 1.2 L of 0.02% (w/v) thimerosal aqueous solution, and filtered. The filtrate was saved, and defined as water-soluble fraction (**WSF**). Sequential extraction of the pellet with 0.05 M CDTA in 0.05 M NaAcO/HAcO buffer

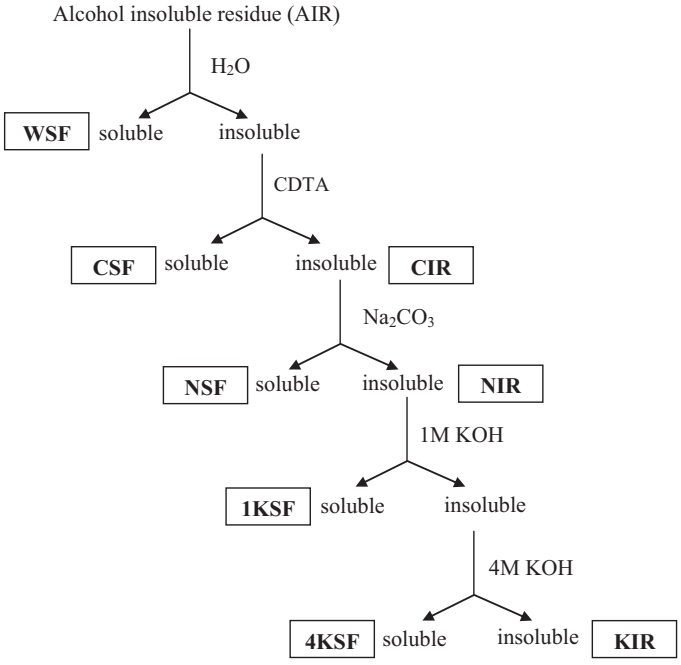

Scheme 1.

(pH 6.0) containing 0.02% (w/v) thimerosal (24 h), 0.1 M Na_2CO_3 in 0.1 mM $NaBH_4$ (24 h), 1 M KOH in 0.1% (w/v) $NaBH_4$ (24 h) and 4 M KOH in 0.1% (w/v) $NaBH_4$ (24 h), produced the CDTA soluble fraction (**CSF**), Na_2CO_3-soluble fraction (**NSF**) and 1 M and 4 M KOH-soluble fractions (**1KSF** and **4KSF**), respectively (Scheme 1). The supernatants were recovered after centrifugation at 13,100 × *g*. In the case of the 1 M KOH- and 4 M KOH-soluble fractions, pH was adjusted to 5.0 with glacial AcOH. All fractions and residues were dialyzed (MW cut-off 6000–8000 Da) exhaustively against tap water for 2 d, and against distilled water for another day at 4 °C, and recovered by lyophilization. Aliquots of the insoluble residues remaining after CDTA, Na_2CO_3 and 4 M KOH extraction steps (**CIR**, **NIR** and **KIR**, respectively; Scheme 1) were isolated after neutralization with AcOH (when necessary), washing with deionized water, dialysis, lyophilization, milling and sieving (ASTM-USA, mesh 100), in order to test their hydration properties.

2.3. General methods

Uronic acids were quantified using the *m*-hydroxybiphenyl method (Filisetti-Cozzi & Carpita, 1991) using GalA as the standard, and expressed as anhydro units. Total carbohydrates were determined by the phenol–H_2SO_4 method (Dubois, Gilles, Hamilton, Rebers, & Smith, 1956) using Glc as the standard. The proportion of neutral sugars (NS) was determined after subtracting the uronic acid content from that of total carbohydrates. For this purpose, the phenol–H_2SO_4 reaction was also carried out with a GalA standard, which showed an absorbance ratio of 0.28 against the same Glc weight. The degree of methylation was calculated as the molar ratio between methanol (determined by the method of Wood and Siddiqui (1971)) and uronic acids. In order to determine the monosaccharide composition, each fraction (ca. 3 mg) was hydrolyzed with 2 M trifluoroacetic acid (TFA, 1 mL) for 90 min at 120 °C in closed-cap vials. The TFA was eliminated by evaporation, and the resulting monosaccharides were reduced using $NaBH_4$ and converted to alditol acetates, which were analyzed using a Hewlett Packard 5890A gas chromatograph fitted with a capillary column 30 m × 0.25 mm i.d. 0.20 μm, SP-2330 (Supelco) and equipped with a FID operated at 240 °C. The injector temperature was 240 °C and

the oven temperature was kept isothermally at 220 °C. Nitrogen was used as the carrier gas at a flow rate of 1 mL/min. Aliquots were injected with a split ratio of ca. 80:1. *Myo*-inositol was used as the internal standard, and the different alditol acetates were identified by comparison with authentic standards. The percentage of the different monosaccharides was calculated by considering that the FID responses are proportional to the molecular weight of the alditol acetates. To obtain the size distributions of polymers and their average molecular weights, 3 mg of **WSF** fractions were dissolved in 1 mL of 0.1 M NaOH. Solutions were cleaned up by centrifugation, and chromatographed on a low-pressure SEC by applying it to a 300 mm × 9 mm i.d. Sepharose CL-6B column eluted at room temperature with 0.1 M NaOH. On the other hand, 3 mg of **CSF** and **NSF** fractions were dissolved in 0.8 mL of 0.4 mg/mL imidazole to which 0.2 mL of 1 M NH_4AcO (pH 5) were added. Solutions were cleaned up by centrifugation, and chromatographed on a low-pressure SEC by applying it to a 300 mm × 9 mm i.d. Sepharose CL-2B column eluted at room temperature with 0.2 M NH_4AcO, pH 5 (Brummell, Dal Cin, Crisosto, & Labavitch, 2004). Fractions were collected and assayed for total carbohydrates. Columns were calibrated with dextrans with molecular weights 40, 80.7 and 500 kDa.

2.4. Determination of cellulose and lignin contents

Hydrolysis of cellulose and non-cellulosic polysaccharides of AIR was performed according to Ng, Parr, Ingham, Rigby, and Waldron (1998) by dispersion of 0.3 g of sample into 2.08 mL of 72% H_2SO_4 for 3 h at room temperature. This dispersion was diluted to make a 1 M H_2SO_4 solution by adding deionized water, and heated at 100 °C for 2.5 h. The dispersions were cooled, centrifuged at 12,000 × *g* for 10 min and the supernatant was separated. The lignin residue was washed three times with deionized water, centrifuged at 12,000 × *g* for 10 min and freeze-dried. A second portion of 0.3 g of sample was dispersed into 72% H_2SO_4 as reported earlier, but dilution to 1 M with water was carried out immediately, and the system was also heated during 2.5 h at 100 °C. The same work-up gave a residue which was considered to be cellulose + lignin. By subtraction of both values, the proportion of cellulose was calculated. The complete assay was carried out in triplicate.

2.5. Cell wall phenolic contents

Phenolics (cell wall phenolic esters, conjugated phenolic acids, and free phenolics) determination was carried out on each AIR (isolated cell wall) sample using the experimental procedure of Bunzel, Ralph, Marita, and Stainhart (2000). Ca. 0.9 g of AIR was mixed with 50 mL of 2 M NaOH for saponification, and left under vacuum and light protection, at room temperature, during 18 h. After acidifying with 9.5 mL of HCl (pH < 2) and stirring for 30 min under vacuum, centrifugation was performed for 15 min at 8000 × *g* (6 °C) and the phenolic content was evaluated in the supernatant using the Folin–Ciocalteu technique reported by Shui and Leong (2006). Gallic acid (Merck, Germany) was used as standard and the results were expressed as mg of gallic acid per 100 g of AIR sample.

2.6. Rheological performance of the isolated cell wall polymers

A sample of 0.04 g of each suitable cell wall polymer fraction was dissolved in deionized water in order to obtain 2.00% (w/w) systems, with aid of vortexing. Then, the solutions were stored at 25 °C for 18 h in order to attain swelling equilibrium as well as for sample resting before measurement. The pH of these sample solutions was ≈6.

2.6.1. Flow assays

Flow curves were determined for those fluid 2.00% (w/w) systems in triplicate at a constant temperature of 20 °C with a rheometer (Paar Physica MCR300, Germany) in the 0.0001–10 rad s^{-1} shear rate ($\dot{\gamma}$) range, after steady-state was reached before recording each data point. Serrated parallel plate geometry of 25 mm-diameter was used, with a gap size of 500 μm. The temperature control was performed in the rheometer through a peltier unit (Viscotherm VT2 Physica, Germany). A viscosity curve recorded over a wide range of shear rate ($\dot{\gamma}$) values is essential to test the fitting of the data points to different viscosity models. In this paper, the Cross model (1) was considered:

$$\eta = \eta_\infty + \frac{(\eta_0 - \eta_\infty)}{1 + (\tau\dot{\gamma})^m} \quad (1)$$

where η_0 represents the zero-shear rate or Newtonian viscosity, τ is the time constant corresponding to the Cross model, and m is a dimensionless constant.

2.6.2. Dynamic oscillatory assays

Mechanical spectra or frequency sweeps performed at linear viscoelastic condition were determined in triplicate at a constant temperature of 20 °C for the 2.00% (w/w) systems that did not flow. Assays were then performed with the rheometer, devices and conditions indicated above, but using oscillatory tests.

Amplitude sweeps were first performed in order to determine the linear viscoelastic range (LVR). Shear storage (G') and loss (G'') moduli as well as strain were recorded as a function of stress, at a constant frequency (0.1 Hz and 10 Hz) and temperature (20 °C). The constant strain value to work in the following frequency sweeps (mechanical spectra) was chosen from the firstly determined LVR for each pectin sample. Each mechanical spectrum was then obtained at a constant strain value selected from the LVR: G' and G'', as well as the tangent of the phase angle ($\tan\delta = G''/G'$), were recorded as a function of increasing angular frequency (ω), after reaching steady-state condition for each point.

Data of G' and G'' versus angular frequency were respectively fitted to a power law-type model (Kim & Yoo, 2006),

$$G' = a \times \omega^b \quad (2)$$

$$G'' = c \times \omega^d \quad (3)$$

where a and c are fitting parameters.

2.7. Hydration properties of the residues

The hydration properties of each insoluble residue remaining after the extraction steps of cell wall polymers with CDTA (**CIR**), Na_2CO_3 (**NIR**) as well as the final residue (**KIR**) of the complete sequential extraction procedure, were measured according to de Escalada Pla, Ponce, Stortz, Rojas, and Gerschenson (2007). Samples were milled and sifted (sieve ASTM-USA, mesh 100) as much as possible.

2.7.1. Swelling capacity (SC)

Each sample of residue (0.2 g) was accurately weighed (to 0.1 mg precision) and placed in a graduated conical tube. After adding 10.00 mL of water, it was allow to hydrate for 18 h at 25 °C. After this time, the final volume attained by the residue was measured (Raghavendra, Rastogi, Raghavarao, & Tharanathan, 2004; Robertson, Monredon, Dysseler, Guillon, and Amadó, 2000). This assay was performed in triplicate for each residue:

$$\text{SC} \quad [\text{mL/g}] = \frac{\text{volume occupied by sample}}{\text{original sample weight}}$$

2.7.2. Water-holding capacity (WHC)

Each sample of residue was accurately weighed (≈1 g) and hydrated in a graduated conical tube with 30.00 mL of water for 18 h at 25 °C. The supernatant was removed and the decanted residue was weighed. The weight of the hydrated residue was recorded (HRW). After freeze-drying, the weight of the dried residue was also recorded (DRW). The WHC was determined in triplicate for each fraction as:

$$\text{WHC}\ \ [\text{g/g}] = \frac{\text{HRW} - \text{DRW}}{\text{DRW}}$$

2.7.3. Water retention capacity (WRC)

The WRC was determined by hydration at 25 °C for 18 h of an accurately weighed sample (≈1 g) of each residue with 30.00 mL of deionized water, into a graduated conical tube. Centrifugation for 30 min at 2000 × *g* was then performed into the same tube. The supernatant was separated and the residue was weighed. The remaining wet fiber was weighed ($R + W_2$), as well as the lyophilized residue (R) (Raghavendra et al., 2004). The WRC was calculated as:

$$\text{WRC}\ \frac{\text{g water}}{\text{g dried residue}} = \frac{W_2}{R}$$

The assay was performed in triplicate for each fraction.

2.7.4. Kinetics of water absorption

Water absorption kinetics was evaluated through measurement of the spontaneous water uptake at 25 °C by an accurately weighed sample (0.02–0.04 g) of the residues, using a modified Baumann capillary device (Robertson et al., 2000). The volume of water absorbed by the sample was measured at different periods of time during 3 h. Kinetic assays were carried out on three samples of each residue. Data were fitted to the following equation and the corresponding parameters were determined:

$$q(t) = \frac{\text{WBC} \times t}{B + t} \quad (4)$$

where q corresponds to the water absorbed at time t, WBC is the maximal water absorption capacity or water binding capacity, and B is the time needed to absorb a half of the maximal water absorption (WBC/2) (Pilosof, 2000).

2.8. Specific volume

The specific volume was determined by weighing with 0.1 mg of precision a measured sample volume in each case (in triplicate), in a 10.00 mL calibrated measuring cylinder.

2.9. Statistical analysis

The results were reported as the average and standard deviation for n sample replicates. Results were analyzed through ANOVA (α: 0.05) followed by multiple comparisons evaluated through least square difference significant difference test, using the Statgraphic package (Statgraphic Plus for Windows, version 5.0, 2001, Manugistic Inc., Rockville, MD, USA). Correlations and nonlinear regressions were performed by using GraphPad Prism 5 (GraphPad Software Inc., USA, 2007).

3. Results and discussion

3.1. Isolation and chemical characterization of cell wall fractions

Two cherry (*P. avium* L.) varieties of contrasting firmness (Regina and Sunburst) at two developmental states were studied. The cell wall polysaccharides (AIR) were sequentially extracted by water, CDTA, Na_2CO_3, as well as by 1 M and 4 M KOH solutions (Scheme 1), and characterized chemically (Table 1).

*3.1.1. Fractions extracted with water (**WSF**)*

The **WSF**s were mostly pectins, as inferred from the presence of large proportions of GalA (48–53%) accompanied by minor proportions of NS (22–31%) (Table 1). Pectic polysaccharides are usually rich in GalA and often contain significant amounts of NS such as rhamnose (Rha), arabinose (Ara) and galactose (Gal) as well as up to other 13 different monosaccharides (Vincken et al., 2003). Three major pectic polysaccharides domains are recognized: the homogalacturonan (HG), displaying linear 4-linked α-GalA chains, the rhamnogalacturonan I (RG-I) constituted by a backbone of alternating Rha and GalA monomers substituted by side chains of arabinogalactans and arabinans, and the more complex rhamnogalacturonan II (RG-II). The chain lengths of the domains can vary considerably, and the sugar composition of RG-I can also show high heterogeneity, whereas RG-II has a highly conserved structure (Willats, Knox, & Mikkelsen, 2006). Water at room temperature extracts the pectin polysaccharides loosely attached to the cell wall material, since this condition preserves covalent and ionic bonds, and β-elimination does not occur (Basanta, Ponce, Rojas, & Stortz, 2012; Fry, 1986). In the present work, the pectin galacturonans of the **WSF**s showed a high degree of methyl esterification (DM = 65–77%) of their carboxylic groups (Table 1). The yield of this fraction increased with ripening. Significantly higher NS/GalA molar ratios were observed for both varieties after ripening (Fig. 1A). On the other hand, the GalA/Rha molar ratio was ≈30 for both unripe cherry varieties (Fig. 1B), which significantly decreased to a half after ripening, suggesting a loss of HG chains of **WSF** at the later developmental stage. The hairy regions of RG-I were constituted by Ara (Ara/Rha between 3.7 and 4.5, Fig. 1C) and some lower Gal molar proportion (Gal/Rha between 2 and 4, Fig. 1D). Minor but significant amounts of xylose (Xyl), mannose (Man) and glucose (Glc) monosaccharides were found in the **WSF**s (Table 1). Polysaccharides extracted by water from the AIR of related stone fruits like Japanese plums (*P. salicina* L.) also presented high proportions of Man (Basanta et al., 2012; Ponce et al., 2010). This may be attributed to the presence of water soluble galactoglucomannans (GGM). In the skin and underlying flesh of fruits like ripe tomato and plum (*Prunus domestica*), some level of mannan transglycosylase activity specific for mannan-based plant polysaccharides like GGM, galactomannan, glucomannan and plain mannan was found by Schröder, Wegrzyn, Bolitho, and Redgwell (2004). Consequently, the Gal content seemed to be distributed between RG-I of the water soluble pectins and GGM. The Xyl content decreased to a half with ripening of both cherry varieties (Table 1). Peña and Carpita (2004) found a similar decrease in the Xyl content of the apple cell walls after ripening. Xylosyl residues may be attached at the *O*-3 positions of the GalA residues to form xylogalacturonans (Peña & Carpita, 2004). The Man content also decreased with ripening, whereas that of Glc increased with ripening.

The average molecular weights (MW) of **WSF**s of both developmental stages of Regina cherry were similar, but the molecular weight distribution increased with ripening (Table 1). On the other hand, the average MW (≈145 kDa) of the water-soluble pectins of unripe Sunburst cell walls was higher than that of Regina. The average MW of the **WSF**-polymers of Sunburst cherry decreased significantly after ripening, while the MW distribution increased noticeably (Table 1).

*3.1.2. Fractions extracted with CDTA solution (**CSF**)*

The **CSF** pectins were significantly enriched in HGs, as inferred from an appreciably higher presence of GalA (64–71%) than NS (12–17%) (Table 1 and Fig. 1A). This result was expected since CDTA

Table 1
Composition, yields, molecular weight and molecular weight distribution of the cell wall polysaccharide fractions extracted by water (**WSF**), CDTA (**CSF**) and sodium carbonate (**NSF**) solutions during sequential extractions from Sunburst (S) and Regina (R) cherry at two ripening states (1, unripe; M, mature).[a]

	WSF				CSF				NSF			
	S1	SM	R1	RM	S1	SM	R1	RM	S1	SM	R1	RM
Yield (% w/w)	2.4 ± 0.2	3.6 ± 1.2	2.0 ± 0.2	3.0 ± 0.2	9 ± 4	4 ± 1	4 ± 2	5 ± 1	26 ± 5	14 ± 2	26 ± 2	17 ± 1
Neutral sugars (% w/w)	22 ± 5	28 ± 1	27 ± 2	31 ± 1	14 ± 2	17 ± 1	12 ± 2	11 ± 4	32 ± 1	34 ± 1	27 ± 2	29 ± 6
Uronic acids (% w/w)	53 ± 1	50 ± 2	52 ± 2	48± 6	64 ± 1	71 ± 4	66 ± 4	69 ± 2	54 ± 2	46 ± 3	52 ± 2	50 ± 4
DM[b] (%)	74	65	72	77	47	51	63	50	18	22	19	21
Molecular weight (kDa)	145	48	39	55 (W[c])	44 (9[d])	29	38	34 (15[d])	34	28	14	13
Half-height width[e] (mL)	6.2	11.3	6.3	7.3	6.1	6.3	5.0	4.6	4.1	8.2	2.6	5.1
Neutral sugar composition (mol/100 mol)												
Rhamnose	7.6 ± 0.4	10.1 ± 0.7	6.4 ± 0.1	8.3 ± 0.1	13.8 ± 0.4	12 ± 2	10 ± 2	13 ± 1	9 ± 2	8.2 ± 0.2	7.4 ± 0.8	8.2 ± 0.9
Fucose	1.0 ± 0.3	1.2 ± 0.2	0.7 ± 0.1	0.8 ± 0.2	3 ± 2	1.0 ± 0.4	0.5 ± 0.7	1.1 ± 0.3	0.4 ± 0.2	0.4	0	0.3 ± 0.4
Arabinose	31.0 ± 0.6	41 ± 5	32.0 ± 0.5	36.4 ± 0.6	64 ± 2	65 ± 5	58 ± 5	66 ± 4	67 ± 5	78 ± 3	69.5 ± 0.1	84 ± 6
Xylose	11 ± 3	7 ± 1	12 ± 1	4.7 ± 0.6	7.7 ± 0.4	3.5 ± 0.3	8.3 ± 0.5	3.7 ± 0.3	1.1 ± 0.5	1.9 ± 0.9	0	1.9 ± 0.8
Mannose	12.6 ± 0.3	9.2 ± 0.3	12.7 ± 0.4	11.1 ± 0.1	4.7 ± 0.6	3 ± 2	3 ± 5	1.7 ± 0.3	0.3 ± 0.4	0.5 ± 0.1	0	0.2 ± 0.4
Galactose	26 ± 2	17 ± 2	24 ± 2	22 ± 1	10.3 ± 2	11 ± 6	11 ± 8	10 ± 5	19 ± 2	8.2 ± 0.3	23.2 ± 0.8	8 ± 2
Glucose	11.7 ± 0.1	14 ± 2	12.9 ± 0.3	16.8 ± 0.7	3 ± 2	3.3 ± 0.2	3 ± 2	3.8 ± 0.1	2 ± 3	2.5 ± 2	0	0.7 ± 0.9

[a] Mean and standard deviations are shown (n = 3–4).
[b] Degree of methyl esterification (DM) expressed as 100 mol of methoxyl group/mol of GalA.
[c] W = wide peak.
[d] A minor peak observed has the molecular weight indicated in parenthesis.
[e] The half height corresponds to the larger peak (when more than one occurs).

selectively extracts HGs electrostatically related through calcium ion bridges (Fry, 1986). The HGs had lower DMs (≈50%) except for the HG extracted from unripe Regina cell walls (63%), but it decreased to 50% upon ripening (Table 1). No major differences in NS/GalA or GalA/Rha ratios were observed for the **CSF**s upon ripening (Fig. 1A and B), but the GalA/Rha molar ratios are larger for the Regina variety (Fig. 1B). It can be assumed that in this variety, the GalA chains of HGs are less frequently interrupted by Rha kinks, which can affect the functional behavior of these pectins (Lapasin & Pricl, 1995; Zsivanovits, MacDougall, Smith, & Ring, 2004). It might be suggested that this high proportion of HG chains present in Regina increases the probability of finding larger Ca-junction zones, which may justify the higher firmness and compactness of Regina cherry. Ca-related pectins are usually localized at the middle lamella between neighboring cells of plant tissue, and especially at tricellular junctions and corners, which are key

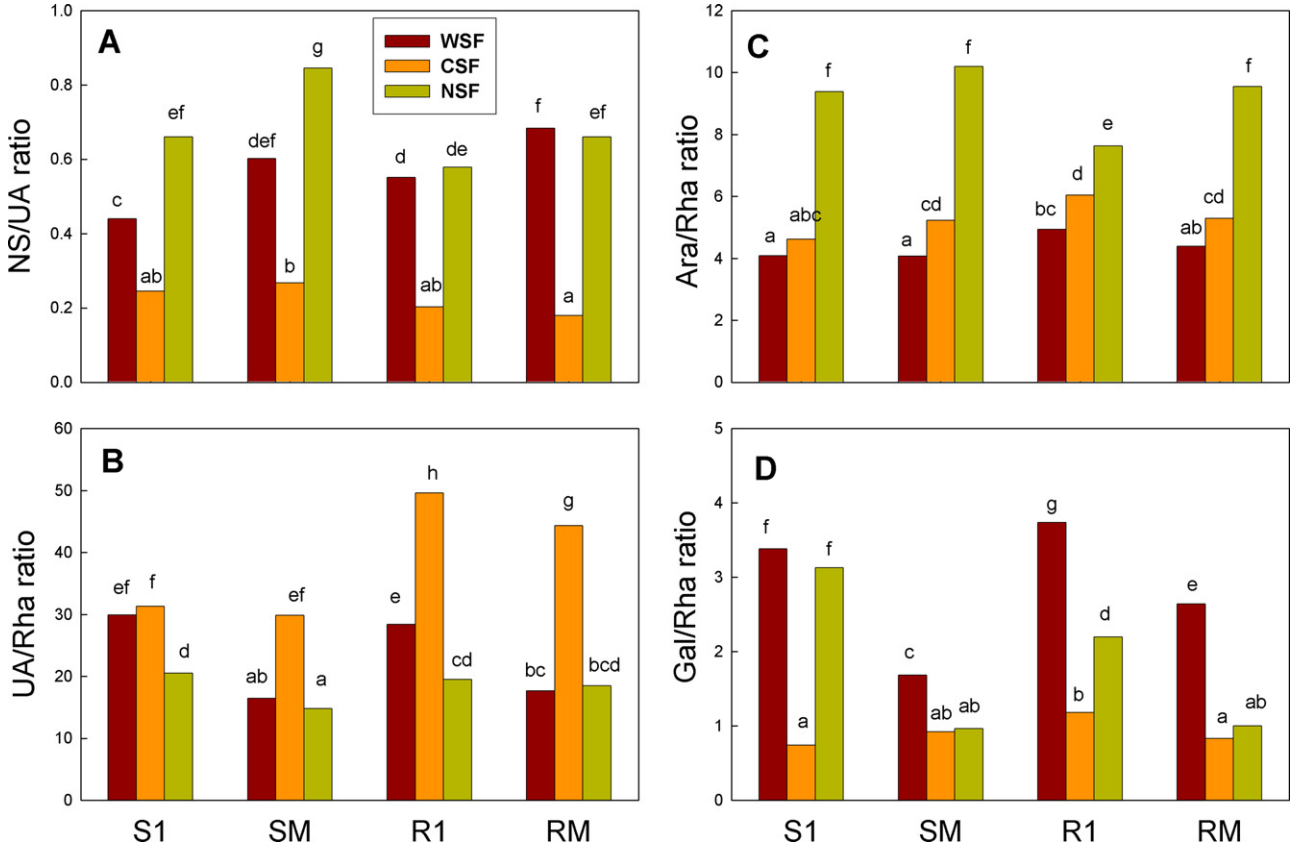

Fig. 1. Molar ratios calculated for neutral sugars/uronic acids (A), uronic acid/rhamnose (B), arabinose/rhamnose (C) and galactose/rhamnose (D) for the **WSF**, **CSF** and **NSF** fractions extracted from Regina (R) or Sunburst (S) cherry cell walls at two ripeness states (1, unripe; M, mature). Different letters indicate significant differences (n = 3–4) based on a Tukey test at a level of significance of $p < 0.05$.

load-bearing locations, all of them responsible for cell-cell adherence and turgor support (Jarvis, 2011; Marry et al., 2006; Vincken et al., 2003). The hairy regions of the RG-I cores in **CSF**-pectins were essentially constituted by Ara, showing lower Gal molar proportions (Fig. 1D). Compared to the **WSFs**, lower though important amounts of Xyl, Man and Glc were also found in all the **CSF**s. The Xyl and Man contents decreased on ripening, as occurred with the **WSF**s (Table 1).

The average MW, and its distribution for the **CSF**s of both cherry varieties were not greatly affected by ripening (Table 1), although the MW distributions of the **CSF**s extracted from Sunburst were higher than those for Regina (Table 1). The **WSF** pectins showed wider MW distributions than the CDTA-extracted polysaccharides (Table 1).

The proportion of Gal is markedly lower than for the **WSF** fractions. Thus, the Gal/Rha ratios decreased notably, whereas the Ara/Rha ratios tended to increase slightly with respect to **WSF**s. This suggests an important increase of the arabinan content in the hairy regions of the RG-I present in the **CSF** fractions.

3.1.3. Fractions extracted with sodium carbonate solution (*NSF*)

Na_2CO_3 solution extracted pectin fractions (**NSF**) covalently bound (Fry, 1986; Marry et al., 2006). Although this fraction is the most abundant for all the AIRs under study, a notable decrease in yield is observed upon ripening (Table 1). The **NSF** pectins showed higher NS/GalA molar ratios for Sunburst than those of the corresponding **WSF**s and **CSF**s, and similar to those of **WSF**s for Regina (Fig. 1A). The NS/GalA molar ratio increased significantly with ripening for Sunburst (Fig. 1A). As expected, low proportion of HG chains appear in the covalently bound pectins, as deduced from their GalA/Rha molar ratios (Fig. 1B). These ratios tend to decrease upon ripening for Sunburst. The RG-I hairy regions of the **NSF** pectins were mainly constituted by Ara, showing the highest Ara/Rha molar ratios (ca. 9) of the current study (Fig. 1C), whereas lower Gal/Rha ratios (1–2) were observed (Fig. 1D). The increase in the molar proportion of Ara/Gal upon ripening is remarkable for the **NSF**-pectins of both varieties, as can be inferred from the Ara/Rha and Gal/Rha ratios appearing in Fig. 1C and D. The Gal/Rha ratios were significantly higher than those of the **NSF**s of immature fruits, but similar for mature samples. Only scarce proportions of Xyl, Man and Glc were found (Table 1) in these fractions.

The average MWs of Regina or Sunburst **NSF** polysaccharides were similar at both respective ripening states, but their distribution increased significantly with ripening (Table 1). The average MWs, as well as the MW-distributions of Sunburst **NSF** pectins were higher than those for Regina (Table 1).

The pectins released by carbonate are usually anchored in the cell wall matrix through covalent bonds, like diester bridges of ferulate (Fry, 1986; Marry et al., 2006), which cross-link arabinan side chains of the RG-I regions of neighboring pectin macromolecules. The Folin–Ciocalteu assay confirmed the existence of phenolic compounds in cherry cell walls. Their content (including possibly ferulate diesters) was 5.00 mg/g AIR (expressed as gallic acid). Hydrolysis of diferulate bridges by Na_2CO_3 to release the cross-linked pectin chains could justify the decrease in MWs observed for the **NSF** pectins (Table 1). Ripening led to a significant increase in the MW distribution, which was usually shifted to lower MWs as in the **WSF**s and **CSF**s. Marry et al. (2006) observed that not only calcium-chelated HG pectin (**CSF**) regions were important in cell-cell adhesion in sugar beet tissue but also feruloyl ester (covalent) bridges, usually removed through Na_2CO_3 treatments. Also, these pectins can cross-link to other components of the cell wall matrix by alkali-labile esters such as galacturonate esters, also hydrolyzed by Na_2CO_3 (Brown & Fry, 1993; Marry et al., 2006). The covalently-bound pectins isolated in the current study constituted 14–26% of the total cell wall polymers, as showed by their yields (Table 1), and represent 65–81% of the total pectin content extracted by water, CDTA and Na_2CO_3 solutions. Pectins rich in RG-I with covalently cross-linked arabinan side chains may be specifically located at the corners of tricellular points, as determined by Marry et al. (2006) for sugar beet tissue.

3.1.4. Cross-linking glycan fractions

After pectin extraction with Na_2CO_3 aqueous solution, only hemicelluloses and cellulose are expected to remain in the residue obtained at this step (**NIR**) (Brett & Waldron, 1996). Strong alkaline solutions (1 M and 4 M KOH) are able to break strong hydrogen bonds and, hence, successively extract the hemicelluloses strongly associated with cellulose (Fry, 1986). Ca. 11–18% of the total cell wall material (AIR) of cherries was extracted by the sequential action of 1 M and 4 M KOH solutions (Table 2). The **1KSF** and **4KSF** fractions carry large amounts of NS (Table 2), predominating over the uronic acid contents (Table 2 and Fig. 2A). The hemicellulose content in the extracted fractions (**1KSF** and **4KSF**) considered as the sum of xylose, glucose and mannose, varied between 26 and 35% of **1KSF** and between 37 and 58% of **4KSF** (Table 2). Gal can also be found as side substituent in hemicellulose macromolecules such as xyloglucans (XG) (Rose & Bennett, 1999). The significant proportions of Xyl, Man, Glc and Gal suggest the presence of XGs and probably some proportion of GGM in cherry cell walls. Xyl was almost constant for both varieties and fraction types, though it decreased sharply upon ripening (Table 2). On the other hand, Man and Glc molar proportions increased in most **4KSF** fractions (Table 2). In all of these fractions, Ara was the main neutral sugar, although its proportion decreased in **4KSF** (Table 2). Small but significant amounts of Rha were also found in both **1KSF** and **4KSF** (Table 2), suggesting that pectin molecules were noticeable anchored in the XG-cellulose load bearing network, and that they did so through the arabinan side chains (Peña & Carpita, 2004). The GalA/Rha molar ratios were very low in the KOH-soluble fractions, and decreased further upon ripening (Fig. 2B). This means that almost only RG-I was co-extracted with both hemicellulose fractions, whereas the Ara/Rha ratios prove that mainly arabinan (Fig. 2C) side chains of cherry pectins were physically anchored in the XG-cellulose load bearing network of cherry cell walls, as observed for other fruits (Peña & Carpita, 2004).

3.2. Rheological characterization of water-, CDTA- and Na_2CO_3-soluble fractions

The cell wall polymeric fractions sequentially extracted by water, CDTA and Na_2CO_3 aqueous solution mainly represented loosely-bound (**WSF**), ionically-bound (**CSF**) and covalently bound (**NSF**) pectins, respectively. Given their water solubility, their functional characterization was carried out by studying the rheological behavior in water.

The 2.0% (w/w) aqueous solutions of **WSF** and **CSF** polymers were assayed by recording the steady shear viscosity curves over a range of shear rates ($\dot{\gamma}$, 10^{-4} up to 0.1 or 10 rad s^{-1}). An initial Newtonian plateau was observed at the lowest shear rates and extended to ≈0.01 rad s^{-1} for **WSF** extracted from both ripe cherry varieties or to 0.04 rad s^{-1} for those of the unripe cherries (Fig. 3A). The **WSF** isolated from ripe varieties presented Newtonian viscosity (η_0) values between 10 and 100 Pa s, whereas η_0 values recorded from unripe cherries were significantly lower (≈3 Pa s). For the **CSF**s, the Newtonian plateau extended to lower shear rates (10^{-3} rad s^{-1}) than for **WSF**s (Fig. 3B). The η_0 values of the **CSF**s extracted from ripe varieties (≈1900 Pa s) were also higher than those recorded from the corresponding unripe Regina (50 Pa s) and Sunburst (5 Pa s) cell wall fractions (Fig. 3B and Table 3). At low shear rates, macromolecules interpenetrate each other domains producing rather a sudden change in flow properties, exemplified

Table 2
Composition and yields of the cell wall polysaccharide fractions extracted by 1 M and 4 M KOH (**1KSF** and **4KSF**) at the latter steps of the sequential extractions of cell wall polymers from Sunburst (S) and Regina (R) cherry at two ripening states (1, unripe; M, mature).[a]

	1KSF				4KSF			
	S1	SM	R1	RM	S1	SM	R1	RM
Yield (% w/w)	10 ± 1	7 ± 2	11 ± 1	7 ± 1	7 ± 1	6 ± 2	7 ± 1	4 ± 1
Neutral sugars (% w/w)	17 ± 4	21 ± 1	20 ± 3	25 ± 2	28 ± 2	31 ± 3	32 ± 2	24 ± 1
Uronic acids (% w/w)	10.0 ± 3.0	5.0 ± 1.0	12.0 ± 1.0	5.0 ± 1.0	3.3 ± 0.9	5.0 ± 0.8	3.0 ± 1.0	4.0 ± 0.5
Neutral sugars (mol/100 mol)								
Rhamnose	4.6 ± 0.8	3.7 ± 0.1	3.6 ± 0.8	4.1 ± 0.5	4.1 ± 0.1	5 ± 2	3.8 ± 0.6	5.8 ± 0.8
Fucose	1.3 ± 0.3	1.4 ± 0.1	0.4 ± 0.6	1.2 ± 0.3	2.4 ± 0.5	2.1 ± 0.4	2.5 ± 0.6	1.8 ± 0.6
Arabinose	52 ± 4	49 ± 6	56 ± 3	56.5 ± 0.3	34 ± 2	36 ± 9	27 ± 6	42 ± 2
Xylose	21 ± 3	17 ± 2	24 ± 9	13.4 ± 0.5	24 ± 3	18 ± 3	27 ± 1	13.8 ± 0.4
Mannose	2.3 ± 0.3	5.5 ± 0.1	0.6 ± 0.8	4.7 ± 0.1	6 ± 1	5 ± 3	5.1 ± 0.5	13 ± 4
Galactose	11 ± 8	11 ± 1	9 ± 3	12 ± 1	15 ± 3	20 ± 8	10 ± 4	13.5 ± 0.8
Glucose	7.4 ± 0.6	13 ± 3	6 ± 4	8 ± 3	14 ± 6	14 ± 2	26 ± 2	19.4 ± 0.5

[a] Mean and standard deviations are shown (n = 2–4).

by more pronounced increases in both the Newtonian viscosity (η_0) and the shear rate dependence of viscosity. At low shear rates there is enough experimental time to develop new interactions among the initially disrupted intermolecular entanglements (Ross-Murphy, 1994). At higher shear rates, a shear thinning or pseudoplastic behavior can be clearly observed, which onset occurs when the rate of externally imposed motion becomes progressively greater than the rate of formation of new entanglements between hydrated macromolecules (Fig. 3A and B). Therefore, the "cross-link density" of the network is depleted, and viscosity is reduced (Morris, Cutler, Ross-Murphy, Rees, & Price, 1981). Consequently, the timescale of (intermolecular) network rearrangement should be related to intramolecular relaxation times of the macromolecules or, at least, of the whole steady-network. The shear rate value at the onset of the shear-thinning increases as the steady network is more fluid, as can be observed for the **WSF** (Fig. 3A) and **CSF**s (Fig. 3B) extracted from both unripe cherry varieties. The highest dependence was observed on the

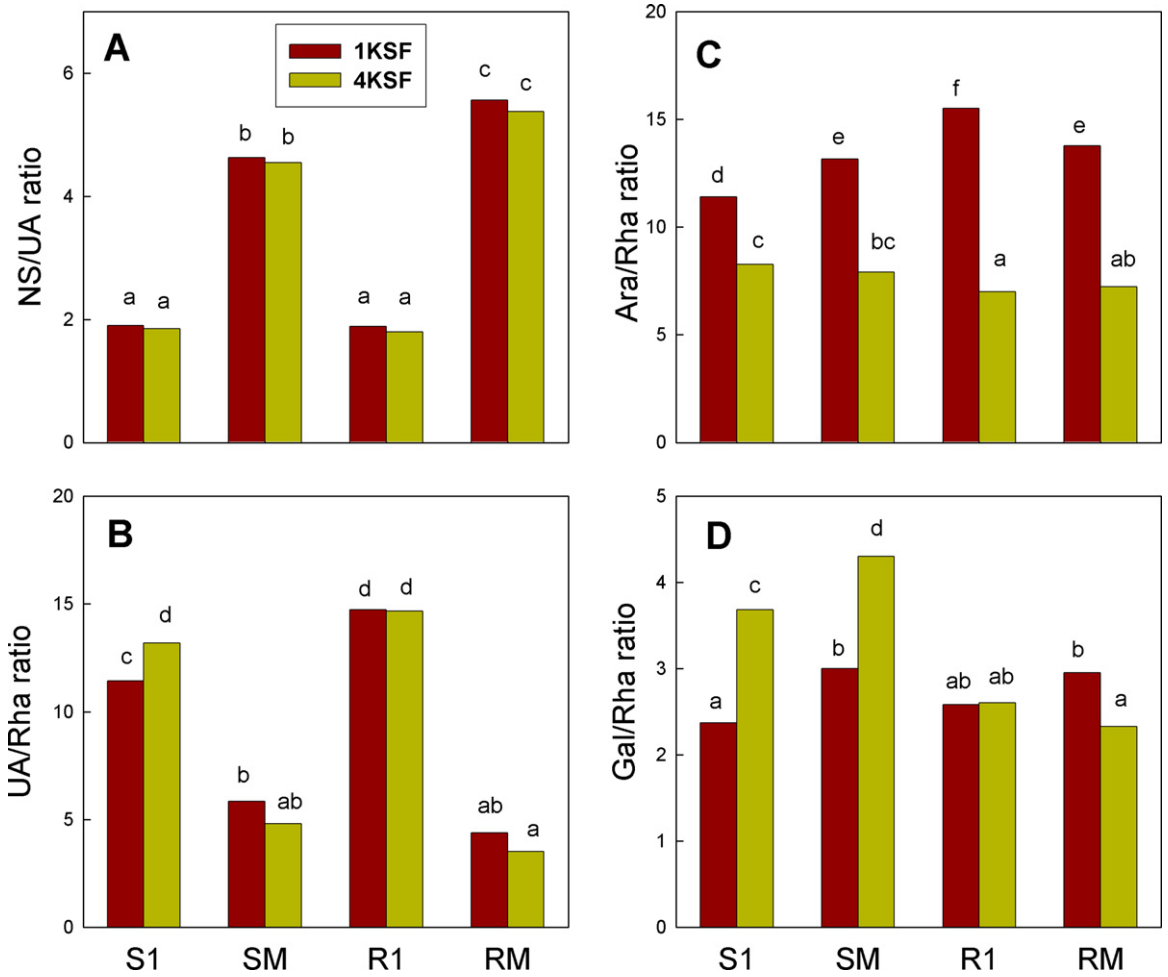

Fig. 2. Molar ratios calculated for neutral sugars/uronic acids (A), uronic acid/rhamnose (B), arabinose/rhamnose (C) and galactose/rhamnose (D) for the **1KSF** and **4KSF** fractions extracted from Regina (R) or Sunburst (S) cherry cell walls at two ripeness states (1, unripe; M, mature). Different letters indicate significant differences (n = 3–4) based on a Tukey test at a level of significance of $p < 0.05$.

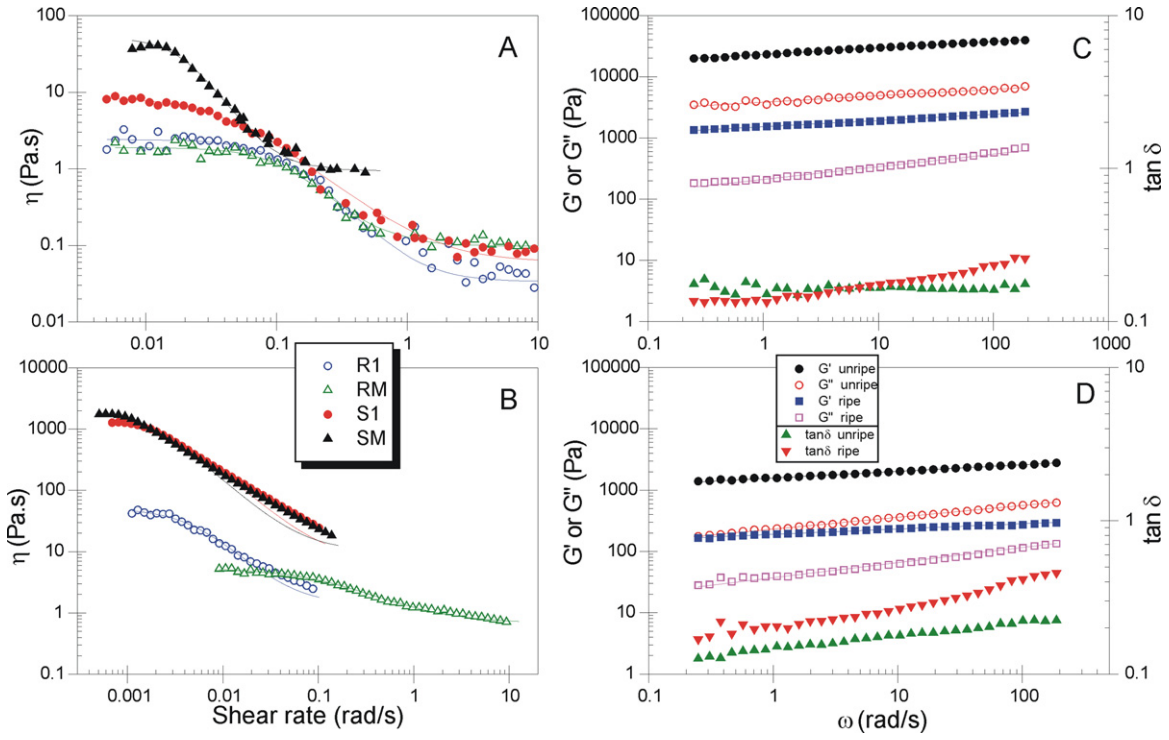

Fig. 3. Flow curves recorded for the fractions extracted from unripe and ripe Regina (**R1** and **RM**), and Sunburst (**S1** and **SM**) cherries: (A) **WSF** and (B) **CSF**. Mechanical spectra obtained from 2.0% (w/w) aqueous solution of the **NSF** fractions extracted from unripe and ripe (C) Regina (**R1** and **RM**), and (D) Sunburst (**S1** and **SM**) cherries. The continuous lines correspond to fitting from experimental points obtained in triplicate (Cross model for A and B).

Table 3
Cross[a] and power law-type[b] model parameters[c] determined after fitting of experimental data respectively obtained through steady-flow and shear dynamic assays (20 °C) from 2.0% (w/w) aqueous solutions of the cell wall polymers extracted with water (**WSF**), CDTA (**CSF**) or sodium carbonate solution (**NSF**) from Sunburst (S) and Regina (R) cherry at two ripening states (1, unripe; M, mature).

Cherry	η_∞ (Pa s)	η_0 (Pa s)	τ (s)	m	R^2
WSF					
S1	0.10 ± 0.05	1.88 ± 0.06	8.3 ± 0.7	1.9 ± 0.3	0.958
SM	0.9 ± 0.2	52 ± 3	51 ± 3	2.6 ± 0.2	0.992
R1	0.03 ± 0.02	2.40 ± 0.07	8.7 ± 0.7	1.6 ± 0.2	0.956
RM	0.06 ± 0.03	8.8 ± 0.2	23.7 ± 0.9	1.40 ± 0.06	0.995
CSF					
S1	0.68 ± 0.05	5.3 ± 0.1	7.0 ± 0.5	1.03 ± 0.07	0.992
SM	10 ± 4	2221 ± 57	631 ± 28	1.47 ± 0.05	0.956
R1	1.4 ± 0.4	51 ± 2	203 ± 14	1.6 ± 0.1	0.990
RM	7 ± 0.9	1581 ± 30	411 ± 14	1.42 ± 0.04	0.998

	a	b exponent	R^2
NSF G' (Pa)			
S1	1582 ± 6	0.108 ± 0.001	0.997
SM	190 ± 1	0.087 ± 0.002	0.985
R1	23,099 ± 86	0.105 ± 0.001	0.997
RM	1525 ± 6	0.101 ± 0.002	0.994
	c	d exponent	R^2
NSF G'' (Pa)			
S1	232 ± 1	0.193 ± 0.002	0.998
SM	37 ± 1	0.247 ± 0.009	0.968
R1	3821 ± 47	0.106 ± 0.004	0.965
RM	210 ± 3	0.206 ± 0.005	0.986

[a] η_0 represents the Newtonian viscosity or the viscosity at zero shear rate; η_∞ represents the infinite or residual viscosity, τ is the time constant and m is a dimensionless parameter.
[b] For the **NSF** fractions.
[c] Mean and standard errors are shown ($n = 3$). R^2: goodness of fit.

shear rate along the shear-thinning range for the **WSF** extracted from ripe Sunburst cell walls (Fig. 3A) and for the **CSF**s extracted from ripe Regina and Sunburst (Fig. 3B) as steady intermolecular entanglements or macromolecular associations were more stable. In other words, a more stable network constituted by the hydrated polysaccharides needs more time for relaxation, which is not possible when shear rate increases after its corresponding onset value. This fact can also be elicited from the values of the structural relaxation time τ obtained by fitting of experimental data to the Cross model (Eq. (1)), in order to obtain rheological parameters (Table 3) for sample comparison. The adjusted model is shown as a continuous line for each curve (Fig. 3A and B). The highest τ value corresponded to the **CSF**s isolated from ripe Regina and Sunburst cell walls, and decreased sharply for the **CSF** of unripe fruit. For the **WSF**s, higher values of τ also corresponded to extracts from ripe cherries (Table 3). Even in the absence of Ca^{2+}, the **CSF** pectins were more structured in water, more able to self interact through overlapping and entanglements. The polymer interactions were less transient than those developed into the **WSF** solutions. The upper Newtonian plateau of the third zone at the highest shear rates, which corresponds to the residual or infinite viscosity (η_∞), was experimentally inaccessible for the most structured **CSF**s (Fig. 3B) but observable for all **WSF** solutions (Fig. 3A).

Pectin polymers self interact in water through non-covalent bonds (hydrogen bonds, hydrophobic and electrostatic interactions). The degree of thickening provided by a polysaccharide is dependent on its chemical composition, macromolecular structure and concentration. Its viscosity is directly related to fundamental molecular properties, i.e. molecular configuration, molecular weight and molecular weight distribution, intramolecular and intermolecular interactions (Lefebvre & Doublier, 2005). The average demethylated block size of HG and the pattern of distribution of demethylated blocks are biologically (or can in vitro be) managed by the blockwise action of pectin methyl esterase, producing pectins with different hydration properties (Zsivanovits

et al., 2004), rheological performance and calcium reactivity, even though they have the same DM (Cameron, Luzio, Vasu, Savary, & Williams, 2011; Guillotin et al., 2005; Willats et al., 2006). The **WSF**-pectins showed wider MW distributions than the **CSF**s (Table 1). The latter characteristic, as well as the higher proportion of HG chains in the **CSF** pectins can be associated with their higher thickening effect upon hydration and dissolution. GalA chains of the Regina HGs are less frequently interrupted by Rha kinks in the **CSF**s, enhancing the rheological behavior of HG-enriched pectins (Lapasin & Pricl, 1995). RG-I cores constitute points of random coil whereas HG chains are semi-flexible polymeric structures (Morris, Ralet, Bonnin, Thibault, & Harding, 2010).

The 2.0% (w/w) systems constituted by dissolution of the **NSF**s (covalently-bound pectins) in water (pH ≈ 6.7) did not flow at room temperature. Hence, these systems were evaluated through oscillatory assays. The mechanical spectra recorded in three frequency decades corresponded to true biopolymer gels, where G' was above G'' in almost one log cycle and the moduli showed a slight dependence on frequency (Lefebvre & Doublier, 2005), as shown in Fig. 3C and D. The latter behavior was characterized through the fitting ($p < 0.001$; $\alpha = 0.05$) of the experimental data to a power law-type model (Eqs. (2) and (3), Kim & Yoo, 2006) and the parameters obtained for sample comparison were reported in Table 3. The shear elastic modulus (G') decreased 8–15 times (Table 3) with ripeness for the **NSF** systems of both varieties, as demonstrated by comparison between the values obtained for "*a*" parameter (Eq. (2)). The G' obtained from the **NSF**-polysaccharides of ripe Regina were of the same order of magnitude of that of unripe Sunburst. The G' profiles showed similar frequency dependence as indicated by the "*b*" exponent (Table 3). On the other hand, G'' was one order of magnitude lower than G' (Fig. 3C and D) as also shown by the "*c*" parameter (Eq. (3)) values (Table 3). As shown by higher values of "*d*" exponent (Eq. (3)), the G'' pattern was significantly more dependent on frequency than G' except for unripe Regina **NSF** polysaccharides (Fig. 3C and D, Table 3). The mechanical spectra obtained were also in agreement with the higher firmness and compactness of Regina cherry.

Na_2CO_3 solution extracted covalently bound pectin fractions (**NSF**) (Fry, 1986; Marry et al., 2006). As stated before, **NSF** pectins showed higher NS/GalA molar ratios for unripe and ripe Sunburst than those of the corresponding **WSF**s and **CSF**s (Fig. 1A), whereas this ratio increased significantly with ripening for both varieties (Fig. 1A). It can be suggested that when the NS/GalA molar ratio increased to 0.6 or more, the elastic contribution was reduced with ripening, as supported by the mechanical spectra of pectin gels (Fig. 3C and D). At the same time, the GalA molar proportion with respect to Rha for **NSF**-pectins significantly decreased with Sunburst ripening to the lowest value found (Fig. 1B). A molar ratio of GalA/Rha ≤ 15 may correspond to lower elastic contribution with respect to the viscous one in the gel microstructure developed by **NSF** pectins (Fig. 3C and D). These pectins were enriched in the RG-I domain with respect to the remaining soluble fractions previously studied. These regions were mainly constituted by Ara, showing the highest Ara/Rha molar ratios (ca. 9) of the current study (Fig. 1C). Only **NSF** pectins from ripe Regina showed comparable Ara/Rha molar ratio. It is suggested that the high proportion of Rha kinks (random coils of RG-I hairy regions) interrupting the HG (semiflexible) chain sequences in conjunction with the high appearance of Ara side chains at the RG-I, may produce the highest macromolecular interactions, leading to gelling. It has been reported that arabinan side chains contribute to modulate the cell wall stiffness by preventing electrostatic calcium mediated interactions at demethylated blocks of the HG chains, thus keeping cell wall flexibility (Jones, Milne, Ashford, & McQueen-Mason, 2003; Moore, Farrant, & Driouich, 2008).

Differences observed in the viscoelasticity of the physical gels produced by the **NSF**s may be mainly attributed to: (a) the differences in the MW distribution, (b) to higher NS/GalA and Ara/Rha ratios at the RG-I cores, as well as to lower GalA/Rha ratios. The NS/GalA molar ratio involves higher (and probably the adequate) proportion of RG-I with respect to HG for the rheological performances observed in Fig. 3C and D.

3.3. Hydration properties of the residues

The insoluble residues remaining after each sequential extraction step performed with CDTA (**CIR**), Na_2CO_3 (**NIR**) and 4 M KOH (**KIR**) solutions (Scheme 1) were characterized in their functionality after milling: the specific volume values were between 15 and 35 cm^3/g for all residues except for the final ones (**KIR**) obtained from ripe Regina and Sunburst cherries, which were 55 cm^3/g or higher (Fig. 4A). The specific volume of the final residue increased significantly with ripening for both varieties. The **CIR** residues showed significantly higher specific volume than **NIR**s for both cherry varieties and ripening degrees. The specific volume of the **CIR** and **NIR** increased significantly with ripening for the Regina variety but not for the Sunburst variety.

The swelling capacity (SC), defined as the ratio of the volume occupied by the sample after immersion in excess of water and equilibration (18 h), to the actual weight (Raghavendra et al., 2004), indicates how much the fiber matrix swells as water is absorbed. Loosely associated water is also being considered in this assay. This parameter varied between 20 and 90 g/g and increased significantly in the direction: **NIR**s < **CIR**s < **KIR**s in most cases, without major dependence on ripeness for the former two residues (Fig. 4B). On the other hand, the final residues (**KIR**) determined from ripe cherries showed significantly higher SC values.

The specific volume (cm^3/g) can be used as an indicator of differences in capillary structure. Theoretically, the more porous the system is, the greater amount of water it should take up, assuming a constant chemical composition. In the present work, the SC correlated significantly (Pearson $r = +0.9790$; $p < 0.0001$; $\alpha = 0.05$) with the specific volume. Hence, **CIR**s showed high porosity after dehydration. They contained the covalently bound pectins characterized in the **NSF**s, other pectin molecules isolated with KOH solutions, as well as hemicelluloses, cellulose and lignin. The highest specific volume and SC values were showed by the final residues (**KIR**) of the extraction. Until this final step, all hemicelluloses as well as the remaining arabinan RG-I-enriched pectins anchored to the hemicellulose-cellulose network were extracted (Table 2). The cell walls of Regina and Sunburst were respectively constituted by 17 and 13% of cellulose, as well as by 8% of lignin in both cherry varieties. The **KIR**s were only constituted by cellulose and lignin. This remaining cellulose seemed to relax extensively in order to show these high SC values; besides, it produced a more porous microstructure. Hemicelluloses are attached to cellulose by strong hydrogen bonding in the residue of the carbonate extraction (**NIR**); they may avoid cellulose relaxation leading to lower swelling (Fig. 4B). Also, the presence of hemicelluloses led to a less porous microstructure (Fig. 4A). The decrease of the pectin contents in the **CIR**s and **NIR**s produced a decrease in the corresponding specific volumes and SCs, whereas the removal of hemicelluloses generated a residue (**KIR**) with the highest specific volume and SC after ripening. The **KIR**s obtained from cell walls of unripe cherries, showed similar specific volume (Fig. 4A) and SCs (Fig. 4B) of **CIR**s, which contain pectins. Removal of **NSF** pectins enriched in RG-I and long arabinans side chains anchored in the XG-cellulose network could in part alter the frame characteristics and, hence, the material porosity. It is also suggested that the important specific volume and SCs of the final residues (**KIR**s) can be the result of the two subsequent alkaline treatments with 1 M and 4 M KOH (Scheme 1). Alkaline extraction alters the I_β crystalline structure of cellulose, producing different allomorphs with distinct

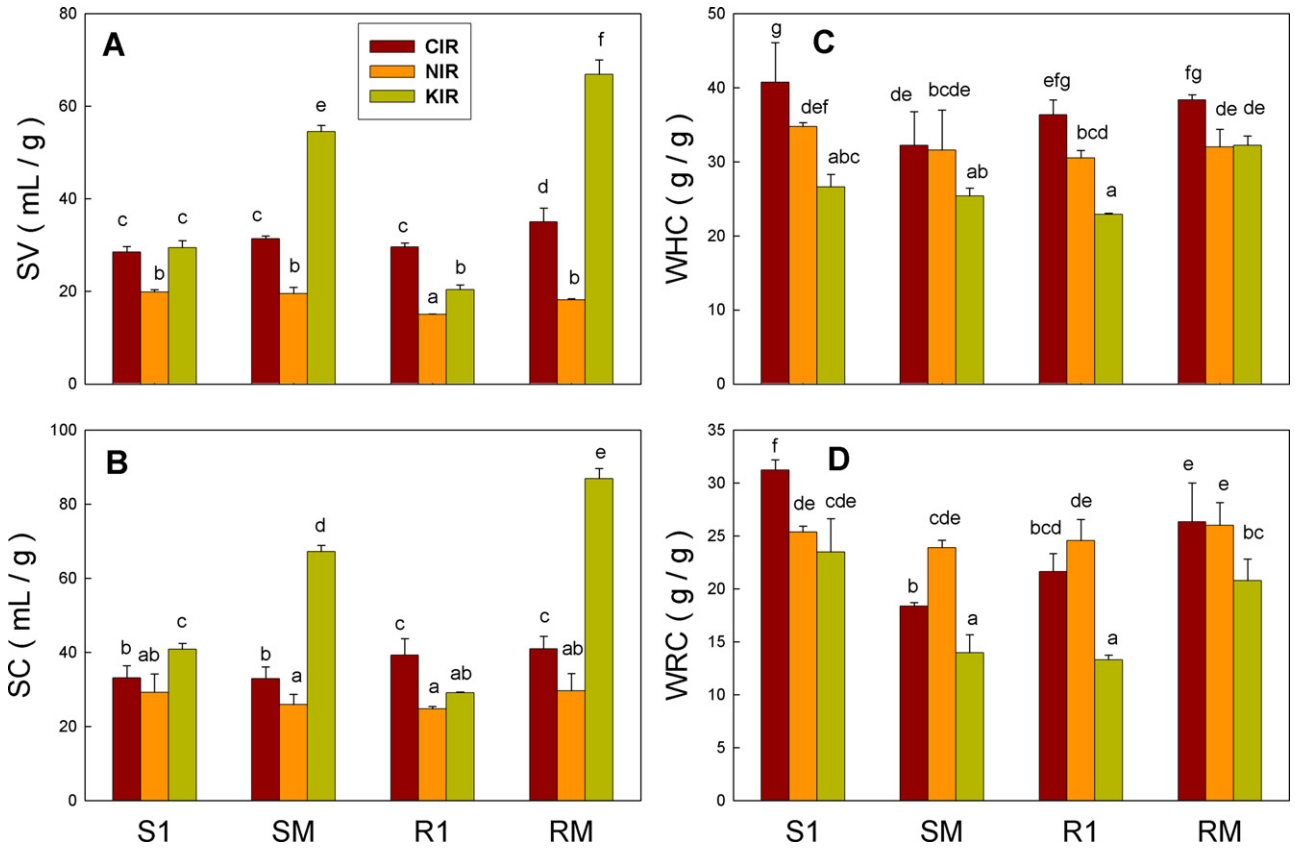

Fig. 4. Specific volumes (A), swelling capacities (B), water holding (C) and water retention capacities (D) determined for the **CIR**, **NIR** and final (**KIR**) insoluble residues. The bars represent mean values ± SD (n = 3–4). Different letters indicate significant differences based on a Tukey test at a level of significance of $p < 0.05$.

hydrogen bonding relationships. It was demonstrated by Mittal, Katahira, Himmel, and Johnson (2011) that the allomorph showed higher digestibility by cellulases.

The water absorption capacity of cell wall polysaccharides is important since it is associated with their biological performance into the cell walls. Besides, cell wall polymers are components of the dietary fiber (Brett & Waldron, 1996) and the water absorption property is an important determinant of stool-bulking effect, which is more related to the manner in which water is held, rather than to the absolute amount held. Strongly-bound water has been found to have no effect on stool weight, whereas loosely-associated water readily increases stool weight (Cadden, 1987). The maximum amount of water that the fiber can hold is a function of its chemical, physical and micro-structural characteristics (Brett & Waldron, 1996; Raghavendra et al., 2004). The water holding capacity (WHC) is defined by the quantity of water retained by the fibers without the application of any external force, except for gravity and atmospheric pressure (Raghavendra et al., 2004). Thus, this parameter also includes the proportion of water loosely associated with the fiber matrix. The WHC varied between 24 and 40 g/g and decreased significantly for both unripe cherry varieties in the direction **CIR**s > **NIR**s > **KIR**s (Fig. 4C), i.e. with their decreasing complexity. Upon ripening, the Regina **KIR** and **NIR** showed the same WHC, whereas Sunburst **CIR** and **NIR** did not differ in their WHC. It can be inferred that high proportions of pectins (as in **CIR**) are associated with higher WHC. The **CIR**s included only pectins covalently related through diferulate ester and anchored to the cell walls through long arabinan side chains. These **CIR** pectins involved 26% of the total cell wall material for both unripe cherry varieties (as calculated from the yields of the **NSF** fractions), and decreased sharply for the **CIR**s obtained from ripe cherries (Table 1).

The water retention capacity (WRC) is defined as the quantity of water that remains into the hydrated fiber following application of an external force such as centrifugation, being then related to strongly-bound water (Raghavendra et al., 2004). The WRC varied between 12 and 31 g/g (Fig. 4D). The WRC values determined for the **KIR**s were the lowest for each variety and ripening degree, except for unripe Sunburst, which did not differ significantly from the WRC values showed by the **NIR** (Fig. 4D). The **CIR** obtained from unripe Sunburst showed the highest WRC. The WRC of **CIR** and **NIR**s did not differ significantly to each other for Regina variety. This hydration parameter was dependent on the cherry variety. Significant correlation (Pearson $r = +0.7841$; $p < 0.0025$; $\alpha = 0.05$) was observed between the WHC and WRC. Higher values of WHC and WRC are related with polysaccharides for which water is a good solvent, that is, polymers able to retain water through hydrogen bonding like pectins. The WHC was always higher than the corresponding WRC value for each variety and ripeness state (Fig. 4C and D).

Water absorption kinetics was determined through the Baumann method and the experimental data were fitted to Eq. (4), yielding the parameters reported in Table 4. The **WBC** parameter tended to decrease following **CIR** > **NIR** > **KIR**. These results agree with those obtained for the WHC and WRC. According to Chen, Piva, and Labuza (1984), fruit fibers, rich in pectins, have a higher WBC than those of the cereal and legume fibers. Pectin molecules self interact in water through non-covalent bonds (hydrogen bonds, hydrophobic and electrostatic interactions). Size and distribution pattern of nonmethylated blocks of HG in pectins contribute to determine different hydration properties (Zsivanovits et al., 2004) and, hence, different functionality (Willats et al., 2006). Besides, the WBC tended to decrease slightly with the ripening degree in cherry residues obtained through sequential extraction of cell wall. The B kinetic parameter indicates the time needed to achieve a half of

Table 4
Kinetic parameters[a] obtained after fitting of experimental data recorded from spontaneous water uptake by the insoluble residues left after the subsequent extraction steps of the CDTA (**CIR**), sodium carbonate (**NIR**) and 4 M-KOH (**KIR**) solutions.

Cherry	**WBC** [b](mL/g)	B^c (min)	R^2
CIR			
S1	18.4 ± 0.5	0.14 ± 0.02	0.785
SM	16.6 ± 0.1	0.117 ± 0.005	0.985
R1	19.7 ± 0.4	0.15 ± 0.02	0.857
RM	16.1 ± 0.3	0.38 ± 0.04	0.867
NIR			
S1	17.6 ± 0.2	0.23 ± 0.01	0.972
SM	14.8 ± 0.3	0.08 ± 0.01	0.872
R1	15.2 ± 0.2	0.092 ± 0.007	0.957
RM	12.4 ± 0.4	0.13 ± 0.03	0.542
KIR			
S1	16.3 ± 0.2	0.30 ± 0.02	0.965
SM	14.2 ± 0.3	0.16 ± 0.03	0.763
R1	13.2 ± 0.3	0.08 ± 0.01	0.839
RM	15.3 ± 0.2	0.073 ± 0.006	0.971

[a] Mean and standard errors are shown ($n = 3$). R^2: goodness of fit.
[b] Water binding capacity, or maximum of spontaneous water uptake at equilibrium.
[c] Time needed to achieve a half of the WBC.

the maximal spontaneous water uptake or WBC. Those B values decreased with the ripening in Sunburst, but increased with the ripening in Regina variety except for the final cellulosic residue (Table 4). Hence, the rate of water absorption (B) was dependent on the variety and degree of ripeness. The final residues (**KIR**) of unripe and ripe Regina absorbed water faster than the rest of the isolated residues (Table 4).

The spontaneous uptake of liquid water by hygroscopic powdered materials on the Baumann apparatus follows a liquid capillary suction mechanism with concomitant swelling (Chen et al., 1984). As soon as the sample is put onto the glass filter atop the water reservoir, water starts to penetrate into the capillary structures of the sample due to "suction" pressure as a result of the surface tension forces of the system. The specific volume (cm^3/g) can be used as an indicator of the differences in capillary structure (de Escalada Pla et al., 2007).

When a dry hydrogel is brought into contact with water, water diffuses into the hydrogel and it swells. Diffusion involves migration of water into pre-existing or dynamically formed spaces between hydrogel chains (Karadağ, Üzüm, & Saraydin, 2002). Diferulate cross-linked pectins through the arabinan side chains, which constitute the CDTA residue (**CIR**), can be considered as a hydrogel-like matrix. More rapid water diffusion into the sample needs, at the same time, the existence of an adequate degree of sample porosity.

Figuerola, Hurtado, Estévez, Chiffelle, and Asenjo (2005) determined SC values between 6.5 and 9 mL water/g (dry mass) and WRC between 1.6 and 2.26 g/g for fiber concentrates made from apple and citrus fruit residues, whereas de Escalada Pla et al. (2007) found SC, WHC and WRC values of 42 mL water/g (dry mass), 43 g/g and 44 g/g, respectively, for the cell wall material isolated from *Cucumis moschata* Duchessne (ex Poiret) pumpkin mesocarp. Vetter and Kunzek (2003) determined the hydration properties of the cell wall material isolated from apple and determined WRC values between 25 and 48 g/g depending on the drying processing, and WBC of ≈22 g/g through the Baumann method. SC of ≈20 mL/g and WRC of ≈17 g/g were determined for the powder of carrot peels (Chantaro, Devahastin, & Chiewchan, 2008).

4. Conclusions

The cell wall matrix of Regina and Sunburst cherry was essentially constituted by covalently bound pectins extractable by Na_2CO_3 solution, probably diferulate cross linked pectins with long arabinan side chains at the RG-I cores. RG-I domains with the longest arabinan side chains were also anchored into the XG-cellulose elastic network of cherry cell walls. Water extractable GGM and xylogalacturonan were also found in the pectin macromolecules, the latter decreased upon ripening.

Ripening of these cherries occurs with an increase in neutral sugars, mainly associated with the actual diminishing in the proportion of HGs. There are optimal NS/GalA and GalA/Rha molar ratios that produce thickening and higher viscosities. It may be inferred that presence of long chains (either of HGs as in CSF or arabinans in NSF) joined to lower molecular weight distribution was associated with higher macromolecule self interactions of pectins and, hence, to higher thickening or gel elastic contribution in water.

The chemical composition and functional properties of cell wall polymers isolated in the soluble fractions, show that the highest firmness and compactness of Regina cherry may be associated with its higher proportion of calcium-bound HGs (**CSF**s) localized in the middle lamellae of cell walls, as well as to some higher molar proportion of NS (Rha and Ara) in the covalently bound pectins extracted by Na_2CO_3 solution (**NSF**s). On the other hand, presence of covalently cross-linked pectins in the residues remaining after the CDTA extraction (**CIR**) of cell wall polysaccharides was associated with better hydration properties. Pectin loss in the residues obtained after the sequential extraction with Na_2CO_3 (**NIR**) and KOH (**KIR**) solutions led to a decrease in the hydration ability, whereas the swelling capacity was related to the specific volume and, hence, to sample porosity. In this sense, alkaline treatments suffered by the final residue (**KIR**) of the complete sequential extraction of cell wall polymers, led essentially to amorphous cellulose, which showed the highest SC in water.

Different chemical and macromolecular structures produced cell wall biopolymers with different functionality. It is known that pectins constitute the cell wall matrix, which is responsible for the viscous drag of the XG–cellulose elastic network. Higher thickening effect of HGs (**CSF**-pectins) and arabinan enriched RG-I (NSF) pectins can significantly contribute to cell wall stiffening and, hence, to the highest firmness of Regina cherry. Cell wall chemical composition and functional properties herein determined can help realize the cell wall behavior in cherry fruit.

Acknowledgements

The help of Agr. Eng. María D. Raffo for picking up the cherries is gratefully acknowledged. This work was supported by grants from University of Buenos Aires, National Research Council of Argentina (CONICET) and Agencia Nacional de Promoción Científica y Tecnológica de la República Argentina (ANPCyT). M.F.B. is a Graduate Research Fellow of CONICET, whereas M.F.E.P., C.A.S. and A.M.R. are Research Members of the same Institution.

References

Andrews, P. K., & Shulin, L. (1995). Cell wall hydrolytic enzyme activity during development of nonclimateric sweet cherry (*Prunus avium* L.) fruit. *Journal of Horticultural Science*, *70*, 561–567.
Barrett, D. M., & Gonzalez, C. (1994). Activity of softening enzymes during cherry maturation. *Journal of Food Science*, *59*, 574–577.
Basanta, M. F., Ponce, N. M. A., Rojas, A. M., & Stortz, C. A. (2012). Effect of extraction time and temperature on the characteristics of loosely bound pectins from Japanese plum. *Carbohydrate Polymers*, *89*, 230–235.
Batisse, C., Buret, M., & Coulomb, P. J. (1996). Biochemical differences in cell wall of cherry fruit between soft and crisp fruit. *Journal of Agricultural and Food Chemistry*, *44*, 453–457.
Brett, C. T., & Waldron, K. W. (1996). *The physiology and biochemistry of plant cell walls* (second edition). London, UK: Chapman & Hall., pp. 26–32.
Brown, J. A., & Fry, S. C. (1993). Novel O-D-galacturonyl esters in the pectic polysaccharides of suspension-cultured plant cells. *Plant Physiology*, *103*, 993–999.
Brummell, D. A., Dal Cin, V., Crisosto, C. H., & Labavitch, J. M. (2004). Cell wall metabolism during maturation, ripening and senescence of peach fruit. *Journal of Experimental Botany*, *55*, 2029–2039.

Bunzel, M., Ralph, J., Marita, J., & Stainhart, H. (2000). Identification of 4-O-5′ coupled diferulic acid from insoluble cereal fiber. *Journal of Agricultural and Food Chemistry*, *48*, 3166–3169.

Cadden, A. M. (1987). Comparative effects of particle size reduction on physical structure and water binding properties of several plant fibers. *Journal of Food Science*, *52*, 1595–1599.

Cameron, R. G., Luzio, G. A., Vasu, P., Savary, B. J., & Williams, M. A. K. (2011). Enzymatic modification of a model homogalacturonan with the thermally tolerant pectin methylesterase from citrus: 1. Nanostructural characterization, enzyme mode of action, and effect of pH. *Journal of Agricultural and Food Chemistry*, *59*, 2717–2724.

Chanliaud, E., Burrows, K. M., Jeronimidis, G., & Gidley, M. J. (2002). Mechanical properties of primary plant cell wall analogues. *Planta*, *215*, 989–996.

Chantaro, P., Devahastin, S., & Chiewchan, N. (2008). Production of antioxidant high dietary fiber powder from carrot peels. *LWT-Food Science and Technology*, *41*, 1987–1994.

Chen, J. Y., Piva, M., & Labuza, T. P. (1984). Evaluation of water binding capacity (WBC) of food fiber sources. *Journal of Food Science*, *49*, 59–63.

Cittadini, E. D. (2007). *Sweet cherries from the end of the world: Options and constraints for fruit production systems in South Patagonia, Argentina*. Ph.D. thesis, Wageningen University, Holland.

de Escalada Pla, M. F., Ponce, N. M. A., Stortz, C. A., Rojas, A. M., & Gerschenson, L. N. (2007). Composition and functional properties of enriched fibre products obtained from pumpkin (*Cucurbita moschata*, Duchesne ex Poiret). *LWT-Food Science and Technology*, *40*, 1176–1185.

Dubois, M., Gilles, K. A., Hamilton, J. K., Rebers, P. A., & Smith, F. (1956). Colorimetric method for determination of sugars and related substances. *Analytical Chemistry*, *28*, 350–356.

Figuerola, F., Hurtado, M. L., Estévez, A. M., Chiffelle, I., & Asenjo, F. (2005). Fibre concentrates from apple pomace and citrus peel as potential fibre sources for food enrichment. *Food Chemistry*, *91*, 395–401.

Filisetti-Cozzi, T. M. C. C., & Carpita, N. C. (1991). Measurement of uronic acids without interference from neutral sugars. *Analytical Biochemistry*, *197*, 157–162.

Fils-Lycaon, B., & Buret, M. (1990). Loss of firmness and changes in pectic fractions during ripening and overripening of sweet cherry. *HortScience*, *25*, 777–778.

Fry, S. C. (1986). Cross-linking of matrix polymers in the growing cell walls of angiosperms. *Annual Review of Plant Physiology*, *37*, 165–186.

Guillotin, S. E., Bakx, E. J., Boulenguer, P., Mazoyer, J., Schols, H. A., & Voragen, A. G. J. (2005). Populations having different GalA blocks characteristics are present in commercial pectins which are chemically similar but have different functionalities. *Carbohydrate Polymers*, *60*, 391–398.

Jarvis, M. C. (2011). Plant cell walls: Supramolecular assemblies. *Food Hydrocolloids*, *25*, 257–262.

Jones, L., Milne, J. L., Ashford, D., & McQueen-Mason, S. J. (2003). Cell wall arabinan is essential for guard cell function. *Proceedings of the National Academy of Sciences of the United States of America*, *100*, 11783–11788.

Karadağ, E., Üzüm, Ö., & Saraydin, D. (2002). Swelling equilibria and dye adsorption studies of chemically crosslinked superabsorbent acrylamide/maleic acid hydrogels. *European Polymer Journal*, *38*, 2133–2141.

Kim, C., & Yoo, B. (2006). Rheological properties of rice starch-xhantan gum mixtures. *Journal of Food Engineering*, *75*, 120–128.

Koh, T. H., & Melton, L. D. (2002). Ripening-related changes in cell wall polysaccharides of strawberry cortical and pith tissues. *Postharvest Biology and Technology*, *26*, 23–33.

Kondo, S., & Danjo, C. (2001). Cell wall polysaccharide metabolism during fruit development in sweet cherry 'Satohnishhiki' as affected by gibberellic acid. *Journal of the Japanese Society of Horticultural Science*, *70*, 178–184.

Lapasin, R., & Pricl, S. (1995). *Rheology of industrial polysaccharides. Theory and applications*. Glasgow, UK: Blackie Academic and Professional, Chapman & Hall., pp. 85–103.

Lefebvre, J., & Doublier, J. L. (2005). Rheological behavior of polysaccharides aqueous systems. In S. Dumitriu (Ed.), *Polysaccharides: Structural diversity and functional diversity* (pp. 357–394). New York, USA: Marcel Dekker.

Marry, M., Roberts, K., Jopson, S. J., Huxham, I. M., Jarvis, M. C., Corsar, J., et al. (2006). Cell–cell adhesion in fresh sugar-beet root parenchyma requires both pectin esters and calcium cross-links. *Physiologia Plantarum*, *126*, 243–256.

Mattheis, J., & Fellman, J. (2004). Cherry (Sweet). In K. C. Gross, C. Y. Wang, & M. Saltveit (Eds.), *The commercial storage of fruits, vegetables, and florist and nursery stocks*. Beltsville, USA: USDA, ARS. Agriculture Handbook Number 66.

Mittal, A., Katahira, R., Himmel, M. E., & Johnson, D. K. (2011). Effects of alkaline or liquid-ammonia treatment on crystalline cellulose: Changes in crystalline structure and effects on enzymatic digestibility. *Biotechnology for Biofuels*, *4*, 41–57.

Moore, J. P., Farrant, J. M., & Driouich, A. (2008). A role for pectin-associated arabinans in maintaining the flexibility of the plant cell wall during water deficit stress. *Plant Signaling and Behavior*, *3*, 102–104.

Morris, E. R., Cutler, A. N., Ross-Murphy, S. B., Rees, D. A., & Price, J. (1981). Concentration and shear rate dependence of viscosity in random coil polysaccharide solutions. *Carbohydrate Polymers*, *1*, 5–21.

Morris, G. A., Ralet, M. C., Bonnin, E., Thibault, J. F., & Harding, S. E. (2010). Physical characterisation of the rhamnogalacturonan and homogalacturonan fractions of sugar beet (*Beta vulgaris*) pectin. *Carbohydrate Polymers*, *82*, 1161–1167.

Ng, A., Parr, A. J., Ingham, L. M., Rigby, N. M., & Waldron, K. W. (1998). Cell wall chemistry of carrots (*Daucus carota* cv, Amstrong) during maturation and storage. *Journal of Agricultural and Food Chemistry*, *46*, 2933–2939.

Peña, M. J., & Carpita, N. C. (2004). Loss of highly branched arabinans and debranching of rhamnogalacturonan I accompany loss of firm texture and cell separation during prolonged storage of apples. *Plant Physiology*, *135*, 1305–1313.

Pilosof, A. M. (2000). Propiedades de hidratación. In A. M. Pilosof, & G. B. Bartholomai (Eds.), *Caracterización funcional y estructural de proteínas* (pp. 17–29). Buenos Aires, Argentina: EUDEBA.

Ponce, N. M. A., Ziegler, V. H., Stortz, C. A., & Sozzi, G. O. (2010). Compositional changes in cell wall polysaccharides from Japanese plum (*Prunus salicina* Lindl.) during growth and on-tree ripening. *Journal of Agricultural and Food Chemistry*, *58*, 2562–2570.

Raghavendra, S. N., Rastogi, N. K., Raghavarao, K. S. M. S., & Tharanathan, R. N. (2004). Dietary fiber from coconut residue: Effects of different treatments and particle size on the hydration properties. *European Food Research and Technology*, *218*, 563–567.

Robertson, J. A., Monredon, F. D., Dysseler, P., Guillon, F., & Amadó, R. (2000). Hydration properties of dietary fiber and resistant starch: A European collaborative study. *LWT-Food Science and Technology*, *33*, 72–79.

Rose, J. C., & Bennett, A. B. (1999). Cooperative disassembly of the cellulose–xyloglucan network of plant cell walls: Parallels between cell expansion and fruit ripening. *Trends in Plant Science*, *4*, 176–183.

Rosli, H. G., Civello, P. M., & Martínez, G. A. (2004). Changes in cell wall composition of three *Fragaria* × *ananassa* cultivars with different softening rate during ripening. *Plant Physiology and Biochemistry*, *42*, 823–831.

Ross-Murphy, S. B. (1994). Rheological methods. In S. B. Ross-Murphy (Ed.), *Physical techniques for the study of food biopolymers* (pp. 343–393). Glasgow, UK: Blackie Academic and Professional, Chapman & Hall.

Schröder, R., Wegrzyn, T. F., Bolitho, K. M., & Redgwell, R. J. (2004). Mannan transglycosylase: A novel enzyme activity in cell walls of higher plants. *Planta*, *219*, 590–600.

Shui, G., & Leong, L. P. (2006). Residue from star fruit as valuable source for functional food ingredients and antioxidant nutraceuticals. *Food Chemistry*, *97*, 277–284.

Toivonen, P. M. A., & Brummell, D. A. (2008). Biochemical bases of appearance and texture in fresh-cut fruit and vegetables. *Postharvest Biology and Technology*, *48*, 1–14.

USDA. (2011). *Stone fruit: World markets and trade foreign agricultural services* (September). http://www.fas.usda.gov/htp/2011StoneFruit.pdf

Vetter, S., & Kunzek, H. (2003). The influence of suspension solution conditions on the rehydration of apple cell wall material. *European Food Research and Technology*, *216*, 39–45.

Vincken, J. P., Schols, H. A., Oomen, R. J. F. J., McCann, M. C., Ulvskov, P., Voragen, A. G. J., et al. (2003). If homogalacturonan were a side chain of rhamnogalacturonan I. Implications for cell wall architecture. *Plant Physiology*, *132*, 1781–1789.

Willats, W. G. T., Knox, J. P., & Mikkelsen, D. (2006). Pectin: New insights into an old polymer are starting to gel. *Trends in Food Science and Technology*, *17*, 97–104.

Wood, P. J., & Siddiqui, I. R. (1971). Determination of methanol and its application for measurement of pectin ester content and pectin methyl esterase activity. *Analytical Biochemistry*, *39*, 418–428.

Zsivanovits, G., MacDougall, A. J., Smith, A. C., & Ring, S. G. (2004). Material properties of concentrated pectin networks. *Carbohydrate Research*, *339*, 1317–1322.